Chen et al., http://www.jcb.org/cgi/content/full/jcb.201201091/DC1

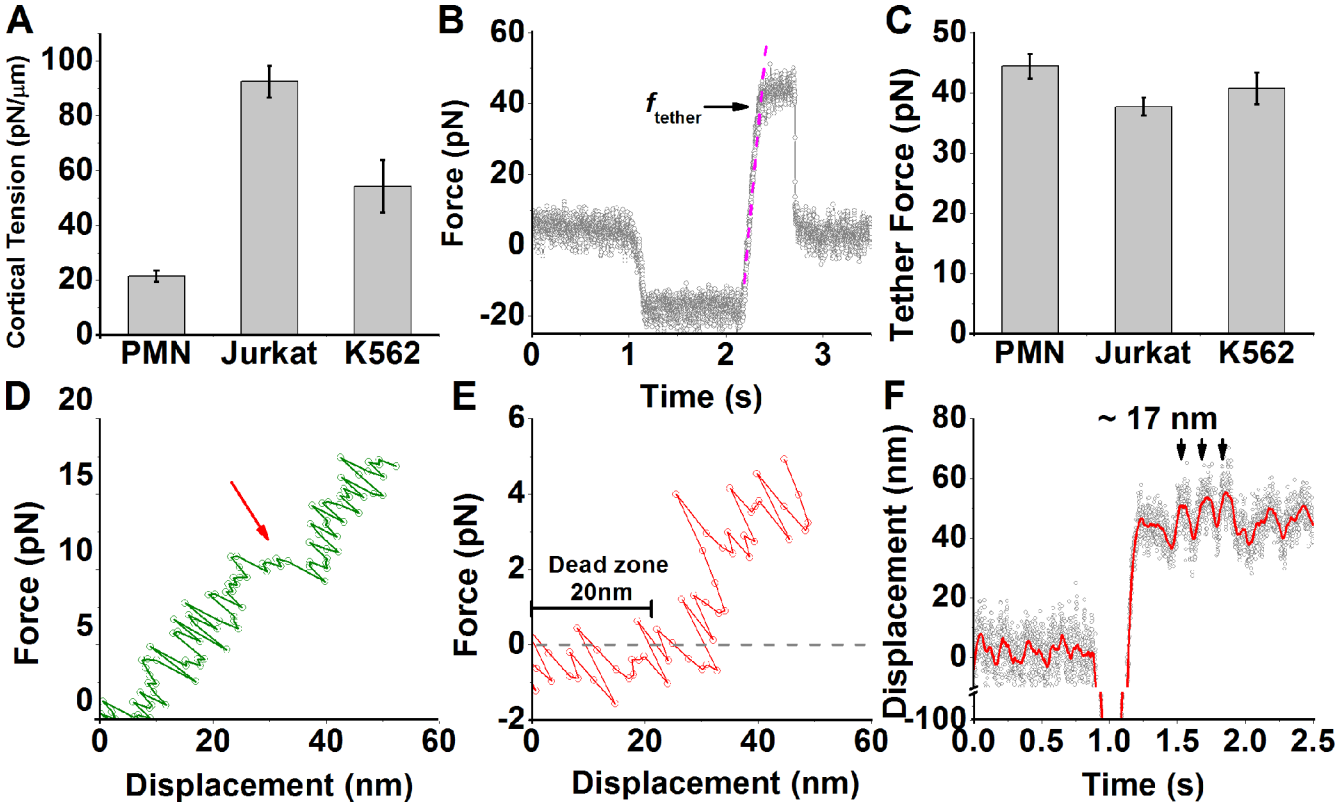

Figure S1. **Cellular mechanical properties, displacement up event during ramping, and multiple up and down events during holding.** (A) Comparison of cortical tensions of three different cells. Error bars represent SEM of >10 measurements. (B) Representative force versus time curve showing the onset of membrane tether extrusion by pulling $\alpha_L\beta_2$ with ICAM-1, which is signified by an abrupt slope drop (indicated) despite that the target cell was continuously being retracted at constant speed (purple dashed line). The tether force f_{tether} is defined as the threshold force required for extruding a membrane tether. (C) Comparison of tether forces for three difference cells. Error bars represent SEM of >30 measurements. (D and E) Representative force versus displacement curves converted from force versus time (e.g., Fig. 1, E and F) and displacement versus time (e.g., Fig. 1, G and H) data but focused on the ramping phase when the target cell was being retracted (compare with Fig. 1 C), showing a sudden displacement increase of ~15 nm, whereas force remained at ~10 pN (D, indicated by an arrow) or ~0 pN (E, dead zone). The former was counted as an up event, whereas the latter was considered a dead zone rather than unbending. The dotted line indicates the zero force level. (F) Multiple up and down events in the holding phase. Representative displacement versus time plot showing three up and down events of ~17-nm displacement change each (indicated by down arrows). The raw data (○) were smoothed (red curve) using the Savitzky-Golay method.

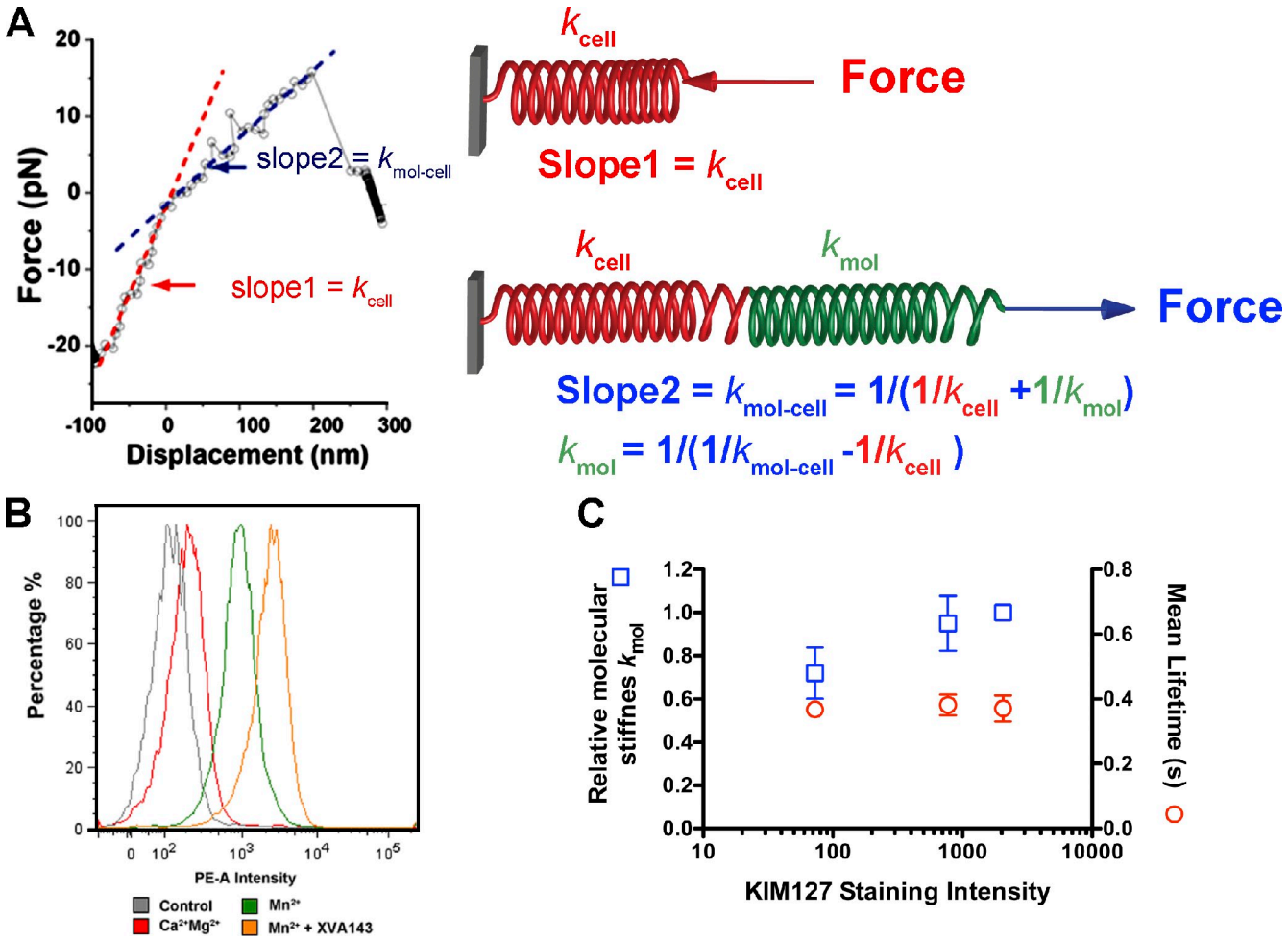

Figure S2. **Measurements of and correlation between molecular stiffness and integrin $\alpha_L\beta_2$ extension in different cation conditions.** (A) Measurement of molecular stiffness by stretch method. Representative force versus displacement data (○) showing a kink in the ascending phase at ~0 pN. The segments below and above the kink correspond to pushing and pulling, respectively, of the target cell against the force probe. The slope of the linear fit to the compressive loading segment (slope 1 of the red dashed line) equals the stiffness k_{cell} of a cellular spring. The slope of the linear fit to the tensile loading segment (slope 2 of the blue dashed line) equals the stiffness $k_{mol-cell}$ of a system that consists of the cellular spring and the molecular spring in series. The molecular stiffness is calculated from $k_{mol} = 1/(1/k_{mol-cell} - 1/k_{cell})$. (B) Measurement of integrin $\alpha_L\beta_2$ conformations in buffers of different cation compositions. Histograms of fluorescence staining of $\alpha_L\beta_2$ on Jurkat cells by KIM127, a reporter mAb for the extended conformation, in 1 mM each of Ca^{2+} and Mg^{2+} (red) or in 1 mM Mn^{2+} without (green) or with (orange) 1 µM XVA143. Gray histogram shows control with an isotype-matched irrelevant antibody. Data were replotted from Chen et al. (2010). (C) Correlation (or the lack thereof) of molecular stiffness or lifetime of $\alpha_L\beta_2$–ICAM-1 bond with the staining of extension reporter mAb KIM127. Means ± SEM (>100 measurements) of molecular stiffness (left ordinate) and lifetime (right ordinate) of $\alpha_L\beta_2$–ICAM-1 bonds measured by the thermal fluctuation method at zero force in 1 mM each of Ca^{2+} and Mg^{2+} or in 1 mM Mn^{2+} without or with 1 µM XVA143 are plotted versus the mean fluorescence intensity of Jurkat cells stained by KIM127 measured in the same cation conditions by flow cytometry (from B). PE-A, phycoerythrin-A.

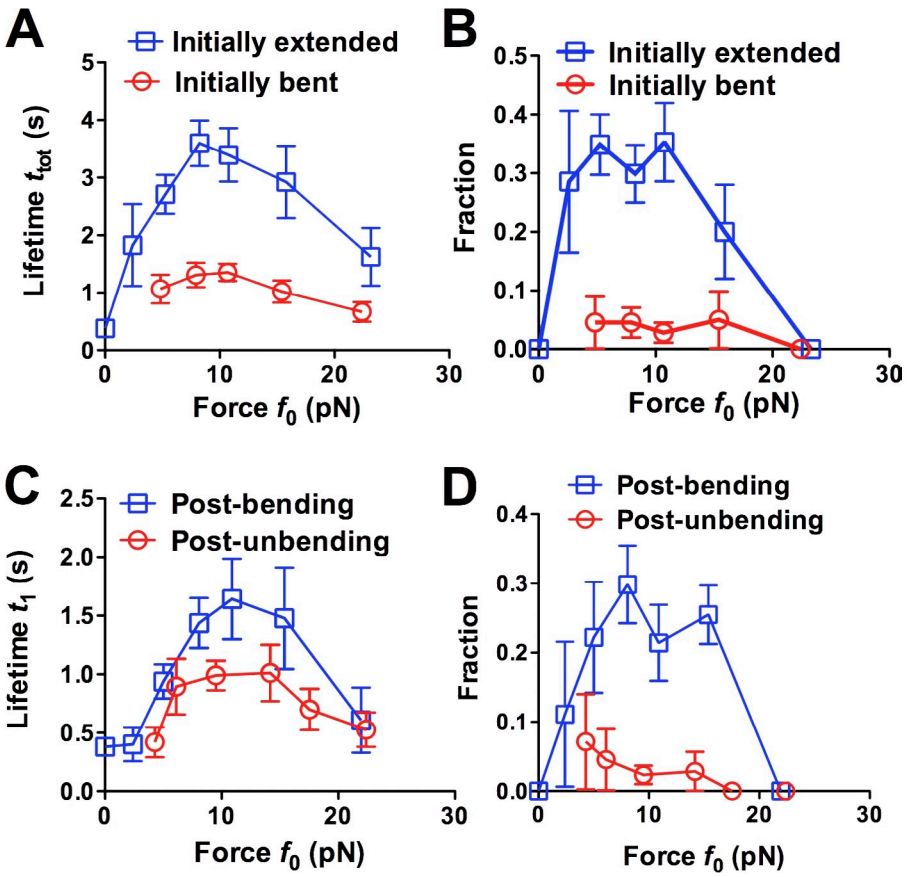

Figure S3. **Effects of initial $\alpha_L\beta_2$ conformations and subsequent change thereof on ligand dissociation under force.** (A and B) Dependence on preswitch force, f_0, of total postclamping short (<10 s) lifetime mean (A) and long (>10 s) lifetime fraction (B) of ICAM-1 bonds with initially extended or bent $\alpha_L\beta_2$ in Mn^{2+} before loading, which underwent a bending or unbending conformational change after loading before dissociation. (C and D) Postbending and postunbending short (<10 s) lifetime mean (C) and long (>10 s) lifetime fraction (D) of $\alpha_L\beta_2$–ICAM-1 bonds versus preswitch force f_0 in Mn^{2+}. Error bars represent SEM of >50 measurements.

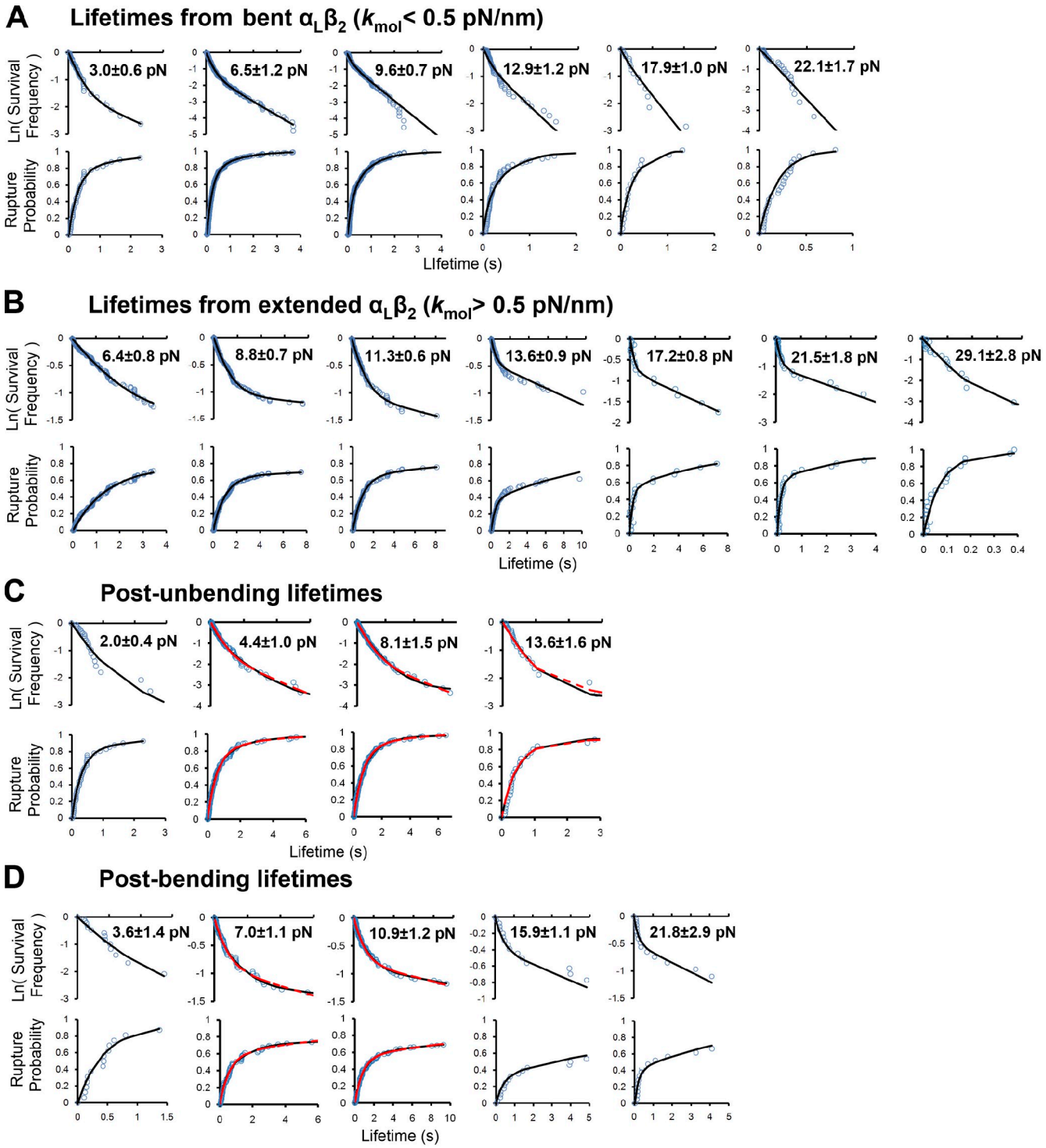

Figure S4. **Analysis of lifetimes of $\alpha_L\beta_2$–ICAM-1 bonds.** Semilog plots of survival frequency (top row of each panel) and rupture probability (bottom row of each panel) versus lifetime data (points) and their three-state (solid black curves) and two-state (solid red dashed curves) model fits of ICAM-1 bonds with soft (k_{mol} < 0.5 pN/nm; A) or stiff (k_{mol} > 0.5 pN/nm; B) $\alpha_L\beta_2$ without unbending or bending in the holding phase or with initially bent (C) or extended (D) $\alpha_L\beta$ after an unbending or bending event in the holding phase measured in Mn^{2+} at the indicated force ranges. Note that some of the red dashed curves are obscured by the overlapping black solid curves. Numbers at the top indicate means ± SD of forces.

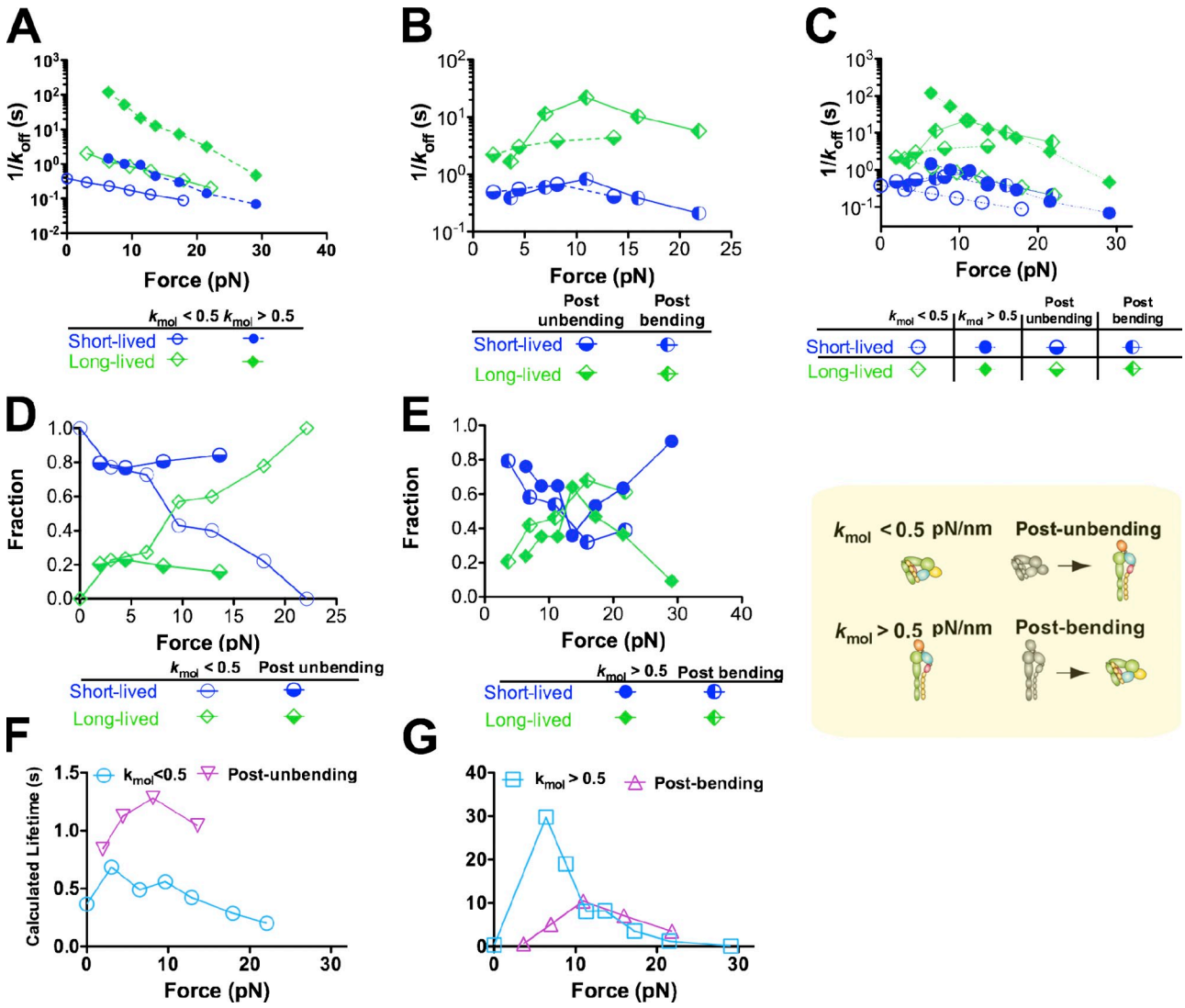

Figure S5. **Two-state model analysis of the effects of bending and unbending of $\alpha_L\beta_2$ on its dissociation from ligand.** (A–E) Force-dependent reciprocal off rates (A–C) or associated fractions (D and E) of the short-lived and long-lived states of $\alpha_L\beta_2$–ICAM-1 bonds evaluated from simultaneously fitting the two-state model to the survival frequency and rupture probability versus lifetime (Fig. S4) without (A) or with (B) bending and unbending measured in Mn^{2+}. All of these reciprocal off rates are superimposed in C, and the fractions are compared in D and E. (F and G) Comparison of calculated mean lifetimes (using parameters obtained from the two-state model fitting) of soft (k_{mol} < 0.5 pN/nm; F) and stiff (k_{mol} > 0.5 pN/nm; G) $\alpha_L\beta_2$–ICAM-1 bonds with the respective postunbending (F) and postbending (G) mean lifetime calculations.

Table S1. **Best-fit Bell model parameters of a three-state or two-state model for the force-dependent reciprocal off rates of the $\alpha_L\beta_2$–ICAM-1 bond in Mn^{2+} for all conditions**

State and state parameters	Short lived		Intermediate lived		Long lived	
	k_0	a/k_BT	k_0	a/k_BT	k_0	a/k_BT
	s^{-1}	pN^{-1}	s^{-1}	pN^{-1}	s^{-1}	pN^{-1}
Without (un)bending (Fig. 6 A) $k_{mol} < 0.5$	2.62	0.08	0.369	0.11	N/A	N/A
Without (un)bending (Fig. 6 A) $k_{mol} > 0.5$			0.278	0.14	0.0026	0.23
With (un)bending (Fig. 6 B) postbending	2.17	0.04	0.33	0.12	0.0046	0.17
With (un)bending (Fig. 6 B) after unbending	1.72	0.06	0.348	0.12	0.0030	0.24
All data (Fig. 6 C)	1.86	0.08	0.322	0.12	0.0032	0.21
Global fitting						
Three-state model	1.82	0.093	0.31	0.13	0.0032	0.22
Two-state model	1.18	0.085	N/A	N/A	0.049	0.12

N/A, not applicable.

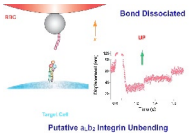

Video 1. **Hypothesizing an up event as $\alpha_L\beta_2$ unbending.** The animated video (produced by Flash [Adobe]; 24 fps) on the left depicts a BFP position-clamp experiment: an $\alpha_L\beta_2$-expressing target cell is driven to contact the ICAM-1–coated BFP probe bead, allow formation of an $\alpha_L\beta_2$–ICAM-1 bond, retract to a desired distance, and clamp at that position for observation of putative $\alpha_L\beta_2$ conformational changes and ICAM-1 dissociation. The data on the right are the same as those in Fig. 1 G but synchronized with the video. The abrupt displacement up event is hypothesized as integrin unbending, as illustrated in the video.

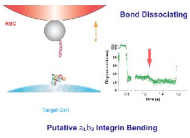

Video 2. **Hypothesizing a down event as $\alpha_L\beta_2$ bending.** The animated video (produced by Flash [Adobe]; 24 fps) on the left depicts a BFP position-clamp experiment: an $\alpha_L\beta_2$-expressing target cell is driven to contact the ICAM-1–coated BFP probe bead, allow formation of an $\alpha_L\beta_2$–ICAM-1 bond, retract to a desired distance, and clamp at that position for observation of putative $\alpha_L\beta_2$ conformational changes and ICAM-1 dissociation. The data on the right are the same as those in Fig. 1 H but synchronized with the video. The abrupt displacement down event is hypothesized as integrin bending, as illustrated in the video.

Reference

Chen, W., J. Lou, and C. Zhu. 2010. Forcing switch from short- to intermediate- and long-lived states of the alphaA domain generates LFA-1/ICAM-1 catch bonds. *J. Biol. Chem.* 285:35967–35978. http://dx.doi.org/10.1074/jbc.M110.155770